

Effects of counter-current driven by electron cyclotron waves on neoclassical tearing mode suppression

Qin Gao(高钦) and Ping-Wei Zheng(郑平卫)

Citation: Chin. Phys. B, 2024, 33 (**5**): 055202. DOI: 10.1088/1674-1056/ad23d3
Journal homepage: http://cpb.iphy.ac.cn; http://iopscience.iop.org/cpb

What follows is a list of articles you may be interested in

Wave field structure and power coupling features of blue-core helicon plasma driven by various antenna geometries and frequencies

Chao Wang(王超), Jia Liu(刘佳), Lei Chang(苌磊), Ling-Feng Lu(卢凌峰), Shi-Jie Zhang(张世杰), and Fan-Tao Zhou(周帆涛)
Chin. Phys. B, 2024, 33 (**3**): 035201. DOI: 10.1088/1674-1056/ad1486

Effects of plasma radiation on the nonlinear evolution of neo-classical tearing modes in tokamak plasmas with reversed magnetic shear

Shuai Jiang(姜帅), Zheng-Xiong Wang(王正汹), Lai Wei(魏来), and Tong Liu(刘桐)
Chin. Phys. B, 2023, 32 (**10**): 105203. DOI: 10.1088/1674-1056/acedf7

Parametric decay instabilities of lower hybrid waves on CFETR

Taotao Zhou(周涛涛), Nong Xiang(项农), Chunyun Gan(甘春芸), Guozhang Jia(贾国章), and Jiale Chen(陈佳乐)
Chin. Phys. B, 2022, 31 (**9**): 095201. DOI: 10.1088/1674-1056/ac67c2

Neoclassical tearing mode stabilization by electron cyclotron current drive for HL-2M tokamak

Jing-Chun Li(李景春), Jia-Qi Dong(董家齐), Xiao-Quan Ji(季小全), and You-Jun Hu(胡友俊)
Chin. Phys. B, 2021, 30 (**7**): 075203. DOI: 10.1088/1674-1056/abfb52

Numerical analysis of the optimized performance of the electron cyclotron wave system in a HL-2M tokamak

Jing-Chun Li(李景春), Xue-Yu Gong(龚学余), Jia-Qi Dong(董家齐), Jun Wang(王俊), Lan Yin(尹岚)
Chin. Phys. B, 2016, 25 (**4**): 045201. DOI: 10.1088/1674-1056/25/4/045201

Effects of counter-current driven by electron cyclotron waves on neoclassical tearing mode suppression

Qin Gao(高钦)[1] and Ping-Wei Zheng(郑平卫)[1,2,†]

[1] *School of Resource Environment and Safety Engineering, University of South China, Hengyang* 421001, *China*
[2] *Demonstration Base for International Science and Technology Cooperation on Nuclear Energy and Nuclear Safety, University of South China, Hengyang* 421001, *China*

(Received 13 October 2023; revised manuscript received 17 December 2023; accepted manuscript online 30 January 2024)

Through theoretical analysis, we construct a physical model that includes the influence of counter-external driven current opposite to the plasma current direction in the neoclassical tearing mode (NTM). The equation is used with this model to obtain the modified Rutherford equation with co-current and counter-current contributions. Consistent with the reported experimental results, numerical simulations have shown that the localized counter external current can only partially suppress NTM when it is far from the resonant magnetic surface. Under some circumstances, the Ohkawa mechanism dominated current drive (OKCD) by electron cyclotron waves can concurrently create both co-current and counter-current. In this instance, the minimal electron cyclotron wave power that suppresses a particular NTM was calculated by the Rutherford equation. The result is marginally less than when taking co-current alone into consideration. As a result, to suppress NTM using OKCD, one only needs to align the co-current with a greater OKCD peak well with the resonant magnetic surface. The effect of its lower counter-current does not need to be considered because the location of the counter-current deviates greatly from the resonant magnetic surface.

Keywords: driven current, neoclassical tearing mode, modified Rutherford equation, electron cyclotron waves

PACS: 52.35.Hr, 52.55.Fa, 52.55.Wq, 52.35.Py **DOI:** 10.1088/1674-1056/ad23d3

1. Introduction

Heating and non-inductive current driven by electron cyclotron (EC) waves are of great significance in the physics and experiments of magnetically confined nuclear fusion plasma. Electron cyclotron current drive (ECCD) at on-axis, off-axis and far off-axis ($r/a > 0.5$) can suppress or actively control some important magnetohydrodynamic (MHD) instabilities in these regions by controlling the current profile of tokamak plasmas.[1]

The far-axis area of tokamak plasma has some significant MHD instabilities,[2] including edge-localized mode (ELM), tearing mode (TM) and neoclassical tearing mode (NTM). The specific pressure, which is the dynamic pressure divided by the magnetic pressure, is severely limited by NTM instability, which can even cause significant disruption of tokamak plasmas. TMs or NTMs may be successfully controlled by the non-inductive current produced by EC waves in the far-axis area.[3,4] ECCD has effectively repressed $3/2$ or $2/1$ NTMs[5–9] in experiments. Low hybrid current drive (LHCD)[10,11] and applied resonant magnetic perturbation (RMP)[12,13] are two further methods of suppressing TMs and NTMs in addition to ECCD. ECCD combined with RMP can also be used to suppress NTMs in tokamak plasma with negative magnetic shear configuration.[14] However, the most successful approach is still ECCD. Two ECCDs are applied in tokamak plasma with negative magnetic shear configuration to control magnetic islands on two resonant magnetic surfaces to reduce the coupling strength between the two modes,[15] hence suppressing NTMs. ECCD will also be used in the future International Thermonuclear Fusion Reactor (ITER) to control these important neoclassical tearing modes.[16]

NTMs are a kind of MHD instability caused by the absence of bootstrap current on the resonant magnetic surface. Replacing the missing bootstrap current by local current drive or heating in the magnetic island can stabilize NTMs.[3] Because the current driven by EC waves is highly localized, it is the most effective way to suppress NTMs by using EC wave to drive non-inductive current in the same direction as plasma current near the O-point of the magnetic island. However, when the deposition position of co-ECCD, which is in the same direction as the plasma current, is significant distance away from the O-point of the magnetic island or the resonant magnetic surface, the effect of inhibiting NTMs is not only very limited,[16–19] but even further promotes the growth of NTM magnetic island.

Although many theories and experiments have focused on the use of co-ECCD to suppress NTMs, counter-ECCD with current direction in the opposite direction to the plasma current has also been used to suppress NTMs.[20,21] Experiments have found that counter-ECCD only partially inhibits NTMs.[20] Of course, suppression or partial suppression of NTMs by counter-ECCD is also conditional. Under the condition of good alignment with the resonant magnetic surface, counter-

†Corresponding author. E-mail: pwzheng@usc.edu.cn

© 2024 Chinese Physical Society and IOP Publishing Ltd

ECCD will not have a suppression effect on NTMs, which is equivalent to the absence of bootstrap current on the target resonant magnetic surface, but will trigger the increase of NTM magnetic island. Therefore, counter-ECCD may have an inhibitory effect on NTMs only when it is not aligned with the resonant magnetic surface. Recent numerical simulation studies show that on a low-aspect-ratio HL-2M tokamak device, the Ohkawa-dominated current drive (OKCD) by EC waves drives co-current and counter-current near the $2/1$ magnetic surface at the normalized radius $\rho \sim 0.6$. The contribution of the co-current to the total driven current is much greater than that of the counter-current. Good alignment of the co-current with the resonant magnetic surface can be used to inhibit $2/1$ NTM.[22] In the presence of co-current and counter-current, if the co-current with a higher amplitude is well aligned with the resonant magnetic surface, the counter-ECCD with a lower amplitude will deviate greatly from the resonant magnetic surface. Therefore, should the wave power required to suppress NTM with both co-ECCD and counter-ECCD be lower than only co-ECCD is considered? How can a suitable model be used to quantitatively evaluate the co-current and counter-current inhibition effect on NTM?

In addition to using the Rutherford equation calculation,[22,23] another method for studying the impact of driving current on NTM magnetic islands is based on MHD simulation.[24,25] Recent simulation studies have found that the conclusions obtained by the two methods are consistent when studying the same problem.[26–28] Using the modified Rutherford equation results in a considerable reduction in computation time. Moreover, the difference in the obtained results between the two methods is also very small. Consequently, in this paper, we choose the modified Rutherford equation for calculations.

The contribution of the counter-ECCD to the growth rate of the NTM magnetic island is added to the original modified Rutherford equation[29] to study the key physical factors affecting the suppression of NTMs by counter-ECCD. The effect of co-current and counter-current generated when EC wave power is deposited at the low-field side on inhibition of 2/1 NTM was quantitatively evaluated.

This paper is divided into four sections. After introducing the research background and motivation, Section 2 constructs a theoretical model based on the modified Rutherford equation. This model includes the contribution terms of co-current and counter-external driven currents by EC waves for the suppression of NTM. In Section 3, the numerical simulation results are presented, and the effects of the peak value of the driven current profile, current profile width, and radial position of the driven current of the counter-driven current on the suppression of NTM are studied. The suppression effect of the co-current and counter-current on NTM is quantitatively studied by coupling the modified Rutherford equation newly constructed in this paper with the ray-tracing program for calculating ECCD. Section 4 summarizes the paper and gives the conclusion.

2. Modified Rutherford equation

In this section, based on reviewing the modified Rutherford equation, we add the contribution term of the counter-current to the evolution of the NTM magnetic island over time and construct a Rutherford equation suitable for the simultaneous presence of co-current and counter-current contributions for our study. The modified Rutherford equation including the contribution of external heating and current drive to the evolution of the NTM magnetic island is[29]

$$0.82\frac{\tau_{\mathrm{r}}}{r_{\mathrm{s}}}\frac{\mathrm{d}w}{\mathrm{d}t} = r_{\mathrm{s}}\Delta_0' + r_{\mathrm{s}}\delta\Delta_0' + r_{\mathrm{s}}\Delta_{\mathrm{BS}}' + r_{\mathrm{s}}\Delta_{\mathrm{CD}}' + r_{\mathrm{s}}\Delta_{\mathrm{H}}', \quad (1)$$

where $\tau_{\mathrm{r}} \equiv \mu_0/\eta$ is the local resistive time for the resistivity η at the rational surface r_{s} of the NTM of interest, and μ_0 is the permeability of free space. The terms on the right-hand side provide the effect of the linear stability index Δ_0', the variation of Δ_0' due to the perturbation of the equilibrium current $\delta\Delta_0'$, the perturbation of the bootstrap current Δ_{BS}', the perturbations of localized non-inductive current drive and the localized heating by EC waves (Δ_{CD}', Δ_{H}'). The first term in Eq. (1) on the right-hand side in this paper is $r_{\mathrm{s}}\Delta_0' = -m$, where m represents the poloidal modulus.

The disturbance term $r_{\mathrm{s}}\Delta_{\mathrm{BS}}'$ is greater than zero, indicating that the lack of bootstrap current causes the width of the NTM magnetic island to grow. According to Refs. [17,29,30], the calculation model is

$$r_{\mathrm{s}}\Delta_{\mathrm{BS}}' = \frac{16\mu_0 L_q r_{\mathrm{s}}}{B_\theta \pi}\frac{4}{3w} f\left(w, W_{\mathrm{marg}}\right) j_{\mathrm{BS}}, \quad (2)$$

where W_{marg} is the critical magnetic island width when the NTM growth rate reaches maximum. In Eq. (2), $f(w, W_{\mathrm{marg}})$ includes the stabilizing effects of two threshold mechanisms, transport and polarization,[31] where $f(w, W_{\mathrm{marg}}) = f_{\mathrm{pol}}(w, W_{\mathrm{marg}}) + f_{\mathrm{tra}}(w, W_{\mathrm{marg}}) - 1$. Here, $f_{\mathrm{pol}}(w, W_{\mathrm{marg}}) = 1 - (W_{\mathrm{marg}}^2/3w^2)$ and $f_{\mathrm{tra}}(w, W_{\mathrm{marg}}) = w^2/(w^2 + W_{\mathrm{marg}}^2)$ describe the stabilizing effects of polarization and transport, respectively. According to the measurement of the plasma beta β (the ratio of plasma kinetic pressure to magnetic pressure) ramp-down experimental boundary conditions, the value of W_{marg} is approximately equal to twice the ion intersection width,[32] $W_{\mathrm{marg}} \approx 2\varepsilon^{1/2}\rho_{\theta \mathrm{i}}$. Here $\varepsilon = r/R$ is the local inverse aspect ratio, r and R are the local minor radius and major radius of the tokamak, respectively. $\rho_{\theta \mathrm{i}} = \left(2m_{\mathrm{i}}k_{\mathrm{B}}T_{\mathrm{i}}/(e^2B_\theta^2)\right)^{1/2}$ is the poloidal radius of gyration of the ion (mass m_{i}), k_{B} is Boltzmann's constant, T_{i} is the ion temperature, B_θ is the poloidal magnetic field size and $L_q = q/(\mathrm{d}q/\mathrm{d}r)$ is the local magnetic shear length.

For the current-driven stability term, ECCD/OKCD mainly suppresses NTMs through two mechanisms. The first stabilizing effect is that ECCD/OKCD replaces the missing bootstrap current in the magnetic island,[17,29]

$$r_s\Delta'_{CD} = -\frac{16\mu_0 L_q}{B_\theta \pi}\frac{\eta_{CD}P_{tot}}{w_{dep}^2} \times F_{CD}\left(w/w_{dep}, x_{dep}, D_{mod}, \phi_{mod}\right), \quad (3)$$

where F_{CD} is the effective parameter to replace the missing bootstrap current, which depends on the ratio of the magnetic island width w to the full width of the driven current profile w_{dep}, $w^* = w/w_{dep}$, the misalignment of co-ECCD/OKCD from target resonant magnetic surface $x_{dep} = r_{dep} - r_s$, the EC wave power modulation duty cycle D_{mod} and the phase deviation φ_{mod} between the power modulation and the O-point of the rotating magnetic island. Under the condition that other factors remain unchanged, $\varphi_{mod} = 0$ is the most beneficial for suppressing an NTM with co-external driven current. Thus, this article only discusses the results under the condition of $\varphi_{mod} = 0$. P_{tot} is the total injected EC wave power given by users, and η_{CD} is the current drive efficiency of EC wave, which can be calculated by the raytracing code. Thus, $\eta_{CD} \times P_{tot}$ is the total current I_{CD} driven by EC wave. If the power deposition and driven current density conform to the Gaussian distribution $\propto \exp[-4/w_{dep}^2]$, then the total driven current is $I_{CD} = \sqrt{k}\pi^{3/2} r_s w_{dep} j_{peak}$, where j_{peak} is the relative magnitude of the local current peak. For elongated plasmas, there is a fitting parameter k that makes I_{CD} approximately equal to the total current calculated by the raytracing code. If the current density profile driven by electron cyclotron waves is close to the Gaussian distribution, the value of k is approximately equal to the tokamak elongation ratio. Since the poloidal cross-section of the tokamak plasma can be approximately regarded as an ellipse, the elliptical area $S = \pi ab = \pi k a^2$, then k is equal to the tokamak elongation ratio b/a. When integrating the ECCD current profile with a Gaussian distribution, the corresponding results can be obtained. Therefore, equation (3) becomes

$$r_s\Delta'_{CD} = -\frac{16\mu_0 L_q r_s}{B_\theta \pi}\frac{\pi^{3/2}\sqrt{k} j_{peak}}{w_{dep}} \times F_{CD}\left(w/w_{dep}, x_{dep}, D_{mod}\right). \quad (4)$$

For co-ECCD/OKCD in the same phase as the magnetic island O-point, $j_{peak} > 0$, to achieve the best suppression effect of NTMs, the misalignment x_{dep} should be as close to zero as possible. This is the so-called well-aligned condition. This is the most critical factor affecting the effective inhibition of NTMs by co-ECCD/OKCD. When misalignment deviation $x \equiv |x_{dep}|/w_{dep} \leq\sim 0.5$, $F_{CD} > 0$, $r_s\Delta'_{CD} < 0$, the co-current has an inhibitory effect on NTMs. Furthermore, when the misalignment deviation is large enough, $x \equiv |x_{dep}|/w_{dep} >\sim 0.5$, $F_{CD} < 0$, $r_s\Delta'_{CD} > 0$, the effect of the co-current will promote the growth of magnetic islands.

The second stabilizing effect of ECCD/OKCD is to improve the classical linear stability. That is to say, the value of $r_s\delta\Delta'_0$ becomes smaller, depending on the relative magnitude of the local current peak j_{peak} by ECCD/OKCD. According to the models in Refs. [29,31], the stability term caused by the external drive current is

$$r_s\delta\Delta'_0 \approx -\frac{4\mu_0 L_q r_s}{B_\theta \pi}\frac{\pi^{3/2}\sqrt{k} j_{peak} D_{mod}}{w_{dep}}\mathrm{erfc}\,(w^*)\,F(x), \quad (5)$$

where, $\mathrm{erfc}\,(x) = \frac{2}{\sqrt{\pi}}\int_x^\infty \mathrm{e}^{-t^2}\,\mathrm{d}t = 1 - \mathrm{erf}\,(x)$ is the complementary error function, $x \equiv |x_{dep}|/w_{dep}$. In the interval $[0,1]$, the zero point of the function $F(x) = 1 - 2.92x + 2.02x^2 - 0.40x^3$ is obtained near $x =\sim 0.5$. The difference from $F(x)$ in Ref. [30] is the full width w_{dep} of the driven current profile of $1/\mathrm{e}$, where e is the nature base number, while the half-maximum width δ_{ec} of the radio frequency current profile EC wave is used in Ref. [32], so that $w_{dep} = \sqrt{\ln 2}\delta_{ec}$. Similarly, for $j_{peak} > 0$ and $x \leq\sim 0.5$, $r_s\delta\Delta'_0 < 0$. In contrast, when $j_{peak} < 0$ and $x >\sim 0.5$, $r_s\delta\Delta'_0 < 0$.

In the presence of both co-current and counter-current in the external-driven current, the modified Rutherford equation for the time evolution of the magnetic island width of NTMs is

$$0.82\frac{\tau_r}{r_s}\frac{\mathrm{d}w}{\mathrm{d}t} = r_s\Delta'_0 + \sum_{i=\pm} r_s\delta\Delta'_{0,i} + r_s\Delta'_{BS} + \sum_{i=\pm} r_s\Delta'_{CD,i} + r_s\Delta'_H, \quad (6)$$

where $i = \pm$ in the second and fourth terms on the right-hand side of Eq. (6) represent the contributions of co-ECCD $(+)$ and counter-ECCD $(-)$ to NTM magnetic island suppression. In the second term on the right-hand side of Eq. (6), $i = +$ represents the contribution term of the co-ECCD. The driving current density should be larger than 0, and the peak position should be well aligned with the resonant rational surface so that NTM can be effectively suppressed; $i = -$ represents the contribution term of counter-ECCD. To suppress NTM, the driving current density should be less than 0, and the peak position should deviate sufficiently from the resonant rational surface. According to the above analysis and discussion, when only the counter-ECCD is considered to suppress NTM, the right-hand side of Eq. (6) does not contain the contribution term of the co-ECCD, and the misalignment deviation $x \equiv |x_{dep}|/w_{dep}$ should be large enough ($x >\sim 0.5$). In this paper, we use the newly constructed modified Rutherford equation to conduct research on the suppression of NTM by the counter-ECCD and quantify the effect of counter-current on

NTM suppression under the Ohkawa dominated current drive (OKCD) of EC wave. In Eq. (6), the details of the effective parameters $F_{\rm CD}$ in $r_{\rm s}\Delta'_{\rm CD}$ and $r_{\rm s}\Delta'_{\rm H}$ are given in Appendix A.

3. Results and analysis

3.1. Results of counter-ECCD to suppress NTM

Co-ECCD that is well aligned with the target resonant magnetic surface can suppress NTM both theoretically and experimentally. Conversely, co-ECCD that is not well aligned with the resonant magnetic surface has less of an inhibitory effect on NTM and may even encourage the formation of NTM magnetic islands. The theoretical analysis in Section 2 suggests that counter-ECCD that veers away from the resonant magnetic surface might hinder NTM. We perform a quantitative investigation into the important elements that determine the suppression of NTM by utilizing counter-ECCD, and we explore the inhibitory effect of counter-ECCD on NTM under different settings. This section is based on the theoretical model presented in Section 2, and it does not address the effect of co-ECCD on NTM. The driven current density ($j_{\rm peak}$), the breadth of the driven current profile ($w_{\rm dep}$) and the relative location of the driven current to the target resonant magnetic surface ($x_{\rm dep} = r_{\rm dep} - r_{\rm s}$) are the primary elements to be considered. As an illustration, consider the low-aspect-ratio HL-2M tokamak, which has the following characteristics: elongation ratio $k = 1.64$, major radius $R = 178$ cm, minor radius $a = 65.5$ cm, central toroidal magnetic field intensity $B_{\rm T} = 2.25$ T, $R/a \sim 2.7$. Table 1 provides further pertinent parameters.

Table 1. Other parameters used in numerical simulations.

$\rho_{2/1}$	$D_{\rm mod}$	L_q (cm)	B_θ (T)	$n_{\rm e}$ (10^{19} m^{-3})	$T_{\rm e}$ (keV)	$j_{\rm BS}$ (A/cm^2)	$\varepsilon_{q=2}$
$0.6025a$	0.5	38.40	0.29	4.10	3.25	19.06	0.22

Figure 1 gives the curve of the NTM magnetic island growth rate as a function of normalized magnetic island width (island width, $w/W_{\rm marg}$). $W_{\rm marg}$ represents the critical magnetic island width when the NTM growth rate reaches maximum. The solid black line in Fig. 1 represents the result without ECCD. In this case, the maximum magnetic island growth rate is $(0.82\frac{\tau_{\rm r}}{r_{\rm s}}\frac{{\rm d}w}{{\rm d}t})^{\rm no\text{-}cd}_{\rm max} = 3.887$. The two dotted lines represent the results under the influence of two typical counter-ECCDs. The peak size $j_{\rm peak}$ of counter-ECCD is -4.2 A/cm^2, and its full width $w_{\rm dep} = 0.03a$. The deviations $x_{\rm dep}$ between counter-ECCD and 2/1 resonance magnetic surface are $0.02a$ and $0.05a$, respectively. Figure 1 shows that when the value of $x_{\rm dep}$ is relatively small, that is, $x_{\rm dep} = 0.02a$, $x \equiv |x_{\rm dep}|/w_{\rm dep} = 0.67$, as shown by the red dotted line in Fig. 1, counter-ECCD does not affect the NTM suppression effect, the maximum growth rate of the magnetic island is larger than the maximum growth rate of 3.887 without ECCD, and it also makes the growth rate larger at different island widths, thus promoting the growth of NTM magnetic islands. When the deviation increases, $x_{\rm dep} = 0.05a$, $x \equiv |x_{\rm dep}|/w_{\rm dep} = 1.67$, as shown by the magenta dotted line in Fig. 1, counter-ECCD shows a partial suppression effect, the growth rate of the magnetic island is significantly reduced in the range of $w/W_{\rm marg} <\sim 2.6$, but when $w/W_{\rm marg} >\sim 2.6$, the growth rate of the magnetic island increases slightly.

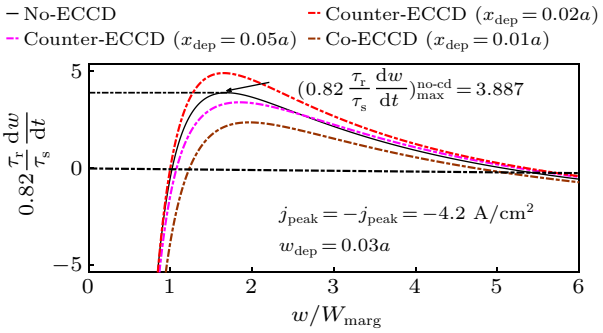


Fig. 1. Curves of magnetic island growth rate versus normalized magnetic island width. The maximum magnetic island growth rate without external driven current is 3.887. The solid black line is the result without an external driven current. The red and magenta dotted lines are the results of counter-ECCD under two misalignment deviations. The tan dotted lines are the results of co-ECCD.

The driving current has an impact on the saturation magnetic island width. The formation of NTM magnetic islands is inhibited by well aligned co-ECCD, as Fig. 1 illustrates, resulting in a reduction in the saturated magnetic island width. However, when the counter-ECCD deviates from the resonant magnetic surface, it is injected into the O-point of the magnetic island. Although it is not particularly obvious, the width of the NTM saturated magnetic island increases slightly, which is not the case with no external drive current.

According to the theoretical model in Section 2, when the misalignment deviation is large enough, $x \equiv |x_{\rm dep}|/w_{\rm dep} >\sim 0.5$, $F_{\rm CD} < 0$, $r_{\rm s}\Delta'_{\rm CD} < 0$, counter-ECCD may have an inhibitory effect on NTM. From the results in Fig. 1, we find that counter-ECCD still has no suppression effect when $x = 0.67$, which may be related to the size of the counter-ECCD $j_{\rm peak}$. The inhibitory effect of counter-ECCD on NTM will be affected by three factors: $j_{\rm peak}$, $x_{\rm dep}$, $w_{\rm dep}$, or be affected by two factors: $j_{\rm peak}$, $x \equiv |x_{\rm dep}|/w_{\rm dep}$.

When we take into account the maximum value of magnetic island growth rate without external ECCD, $(0.82\frac{\tau_{\rm r}}{r_{\rm s}}\frac{{\rm d}w}{{\rm d}t})^{\rm no\text{-}cd}_{\rm max} = 3.887$, different counter-ECCD characteristic parameters ($j_{\rm peak}$, $x_{\rm dep}$, $w_{\rm dep}$) are considered. The range of $j_{\rm peak}$ increases from ~ 1 A/cm^2 to ~ 10 A/cm^2, and the value of $j_{\rm peak}$ is much less than the bootstrap current density ($j_{\rm BS} = 19.06$ A/cm^2) on the 2/1 magnetic surface, which is listed in Table 1, the value of $x_{\rm dep}$ increases uniformly from $0.04a$ to $0.10a$ and the value of $w_{\rm dep}$ increases uniformly from

0.04a to 0.16a. The corresponding maximum magnetic island growth rate $(0.82\frac{\tau_r}{r_s}\frac{dw}{dt})^{cd}_{max}$ under these conditions is calculated, and the results are shown in Fig. 2. Counter-ECCD has an inhibitory effect on NTM if $(0.82\frac{\tau_r}{r_s}\frac{dw}{dt})^{cd}_{max} < 3.887$. It not only has no inhibitory effect, but promotes the growth of NTM magnetic islands.

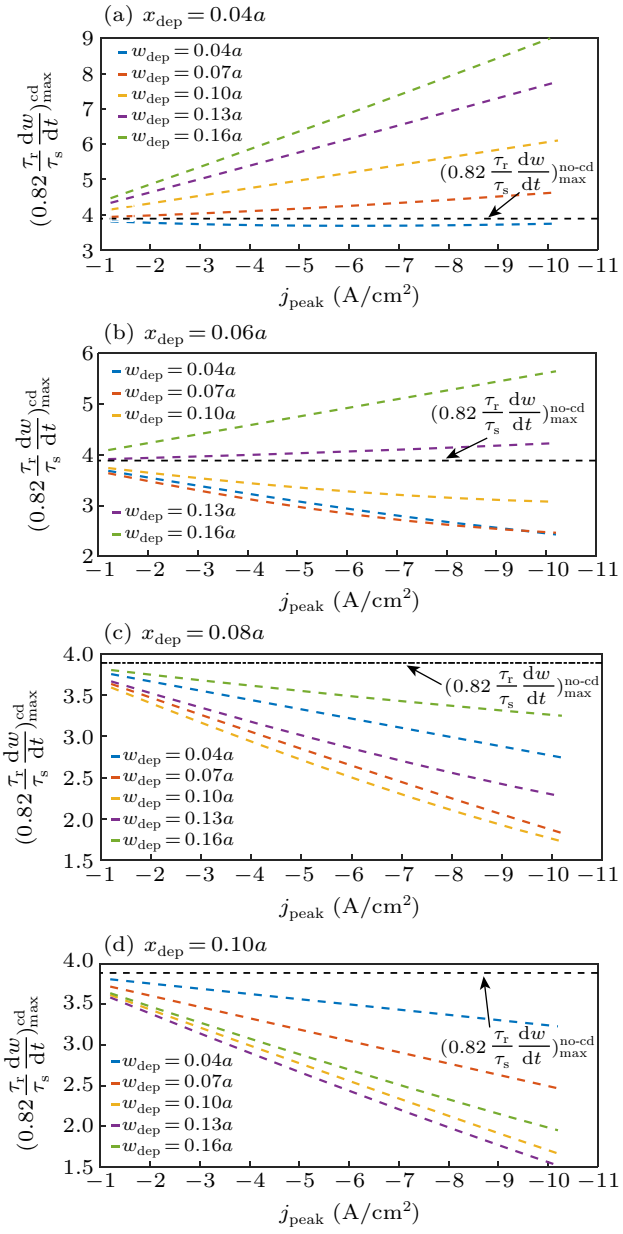


Fig. 2. The influence of counter-ECCD on the maximum magnetic island growth rate of NTM under different characteristic parameters (j_{peak}, x_{dep}, w_{dep}).

Figure 2 shows the effects of w_{dep} and j_{peak} on the maximum growth rate of the magnetic island under the conditions of $x_{dep} = 0.04a$, $0.06a$, $0.08a$ and $0.10a$, respectively. It can be seen from Fig. 2(a) that when the counter-ECCD deposition position deviates from the 2/1 resonant magnetic surface by $x_{dep} = 0.04a$, only $w_{dep} = 0.04a$ has an inhibitory effect. In this case, $x_{dep} > 0.5w_{dep}$, but the inhibitory effect of counter-ECCD is not significant under this condition. When $x_{dep} = 0.04a$ and $w_{dep} \geq 0.07a$, that is, $x \equiv |x_{dep}|/w_{dep} \leq 0.57$, counter-ECCD will promote the growth of NTM magnetic island, and its maximum growth rate increases with the increase in the value of j_{peak} of counter-ECCD. As x_{dep} increases, the inhibitory effect of counter-ECCD on NTM gradually increases. When $x_{dep} = 0.06a$, only counter-ECCD with $w_{dep} \leq 0.10a$ has an inhibitory effect on NTM, while counter-ECCDs with a wider width ($w_{dep} \geq 0.13a$) have no inhibitory effect. In this case, the minimum value of $x \equiv |x_{dep}|/w_{dep}$ is 0.6 for the suppression of NTM by counter-ECCDs. When the misalignment deviation x_{dep} further increases to 0.08a and 0.10a, as shown in Figs. 2(c)–2(d), counter-ECCD can suppress NTM under all given values of w_{dep}, but the inhibitory effect does not increase with the increase in the value of w_{dep}. There is an optimal value of w_{dep}. For $x_{dep} = 0.08a$ and 0.10a, the value of w_{dep} with the best inhibitory effect is 0.10a and 0.13a.

It can be found from Fig. 2 that when the value of (x_{dep}, w_{dep}) makes counter-ECCD have an inhibitory effect on NTM, its inhibitory effect increases as the value of $|j_{peak}|$ increases. Of course, the value of (x_{dep}, w_{dep}) can also make counter-ECCD promote the growth of NTM magnetic islands, as shown in Figs. 2(a)–2(b) where the higher counter-ECCD value will further promote the growth of NTM magnetic islands. Therefore, counter-ECCD will promote the growth of NTM magnetic islands when the value of misalignment deviation x_{dep} is small enough. Only when the value of x_{dep} is large enough, will counter-ECCD have an inhibitory effect on NTM. According to the results in Fig. 2, when the value of the misalignment deviation x_{dep} is between 0.08a and 0.10a and $x \equiv |x_{dep}|/w_{dep} \sim 0.8$, counter-ECCD has a better inhibitory effect on NTM. However, since the maximum value of $|j_{peak}|$ in Fig. 2 is ~ 10 A/cm^2, which is lower than the bootstrap current size $j_{BS} = 19.06$ A/cm^2 of the target resonant magnetic surface, the counter-ECCD inhibitory effect on NTM is only partial. This is also consistent with the experimental results of counter-ECCD inhibiting NTM.[20]

According to the results in Fig. 2, with the suppression effect, the maximum value of the magnetic island growth rate is smaller than the maximum value without driving current. Combined with the results of Figs. 1 and 3, within the partial magnetic island width range, counter-ECCD causes the growth rate of the magnetic island to drop significantly. When the width of the magnetic island is large, counter-ECCD does not make the growth rate of the magnetic island smaller. For example, for $x_{dep} = 0.08a$, $w_{dep} = 0.10a$, $x \equiv |x_{dep}/w_{dep}| = 0.8$, and $|j_{peak}| = j_{BS} = 19.06$ A/cm^2, the effect of counter-ECCD on NTM inhibition is shown in Fig. 3. When the magnetic island width $w/W_{marg} <\sim 3.0$, counter-ECCD has an obvious inhibitory effect on NTM. When $3.0 < w/W_{marg} <\sim 3.8$, the suppression effect will be reduced, while for $w/W_{marg} >\sim$

3.8, there is no suppression effect. In this case, the maximum growth rate of the magnetic island is reduced to ~ 1.6, which shows that under optimized conditions when the peak value of the counter-ECCD is close to the bootstrap current on the resonant magnetic surface, its inhibitory effect on NTM is also partial. The magnetic island can be interpreted as a current filament in the counter-current direction. Therefore, driving co-current in the O-point counterbalances this filament, hence reducing the island growth. In contrast, driving current on the X-point enhances the perturbation induced by the filament and so drives the island growth. In Fig. 2(c), when $x_{\rm dep} = 0.08a$, $w_{\rm dep} = 0.10a$ and $j_{\rm peak} = -10.0$ A/cm^2, the maximum growth rate of the magnetic island is about 1.75. This shows that increasing the peak current of counter-ECCD cannot significantly enhance its NTM inhibition effect.

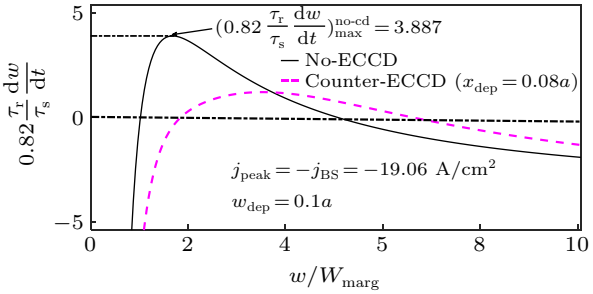


Fig. 3. For $|j_{\rm peak}| = j_{\rm BS}$, the effect of counter-ECCD on NTM suppression, the black solid line is the result without external drive current.

3.2. Results of combining co-current and counter-current to suppress NTM

According to theoretical studies, in the region of normalized radius $\rho = r/a > 0.5$ in tokamak plasma, the far off-axis current can be driven by the electron cyclotron wave's Ohkawa mechanism. In this region, MHD instabilities such as NTM and ELM can be suppressed through OKCD.[22,33–35] It was discovered that when the OKCD deposition position is close to $\rho \sim 0.6$, the OKCD profile will have two driven current peaks. The counter-OKCD peak position is far from the target resonant magnetic surface and has a peak value that is significantly lower than the co-OKCD peak value. In contrast, the co-OKCD peak position is perfectly aligned with the surface.[22] In this section, we use the theoretical model established in this paper to quantitatively calculate the impact of this current distribution characteristic on the suppression of NTM and analyze the effect of this part of the counter-OKCD.

According to Ref. [22], the characteristic parameters of OKCD ($\rho_{\rm ec}$, $j_{\rm CD}$, and $w_{\rm dep}/a$) are calculated by GENRAY code.[36–38] Their values can be changed by adjusting the initial incident angle, toroidal incident angle α and poloidal incident angle β. Adjusting (α, β) so that the co-OKCD peak of the OKCD profile is well aligned with the position of the $2/1$ resonance magnetic surface at $\rho_{2/1} = 0.6025a$. As shown in Fig. 4, the co-OKCD peak is located at $0.6075a$ and the counter-OKCD peak is located at $0.6725a$. The characteristic physical quantities of the co-OKCD and counter-OKCD of the OKCD profile are extracted from Fig. 4, as shown in Table 2. Other physical quantities needed to calculate the minimum power of the EC wave are given in Table 1. Based on these characteristic physical quantities, using the theoretical model in Section 2, it is calculated that the minimum power to suppress $2/1$ NTM when only considering the co-OKCD is $P^+_{\rm min} = 1.18$ MW, while considering both co-OKCD and counter-OKCD, the minimum power is $P_{\rm min} = 1.15$ MW. Figure 5 shows the suppression results of the co-current and counter-current of OKCD on the NTM magnetic island, indicating that both the counter-current far away from the resonant magnetic surface and the well aligned co-current have a suppressive effect on NTM. In this case, due to the higher amplitude of the co-current of OKCD compared to counter-current, the main contribution to NTM suppression comes from the co-current, while the counter-current only has a partial suppression effect.

Table 2. Main parameters of co-current and counter-current in Fig. 4 and the minimum EC power to stabilize $2/1$ NTM.

$\rho_{2/1}$	$j^+_{\rm peak}$ (A·cm^{-2}·MW^{-1})	$j^-_{\rm peak}$ (A·cm^{-2}·MW^{-1})
$0.6025a$	8.4065	−0.8253
$r^+_{\rm dep}/a$	$r^-_{\rm dep}/a$	$w^+_{\rm dep}/a$
0.6075	0.6725	0.055
$w^-_{\rm dep}/a$	$P_{\rm min}$ (MW)	$P^+_{\rm min}$ (MW)
0.045	1.15	1.18

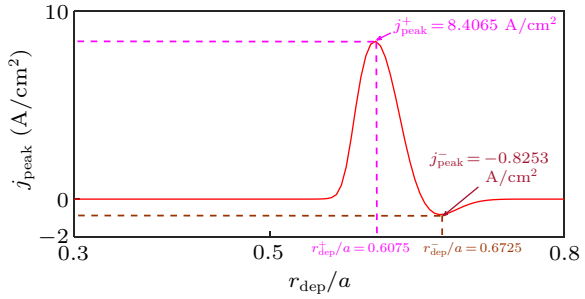


Fig. 4. OKCD co-current and counter-current peak position and value. The driven current profile is calculated by the GENRAY program at 1 MW power.

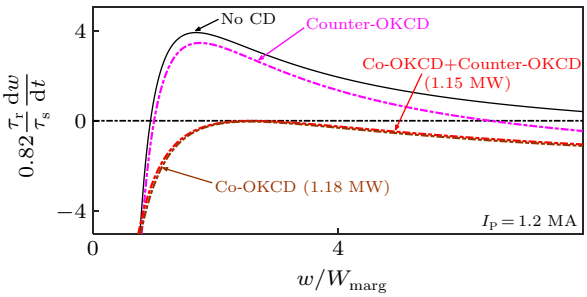


Fig. 5. The suppression effect of co-current and counter-current of OKCD on the NTM magnetic island in Fig. 4.

Table 3. Main parameters of co-current and counter-current of OKCD and minimum EC power for stabilizing 2/1 NTM at different initial incident angles.

α (°)	β (°)	$j^{+}_{\rm peak}$ (A·cm^{-2}·MW^{-1})	$j^{-}_{\rm peak}$ (A·cm^{-2}·MW^{-1})	$r^{+}_{\rm dep}/a$	$r^{-}_{\rm dep}/a$	$w^{+}_{\rm dep}/a$	$w^{-}_{\rm dep}/a$	$P_{\rm min}$ (MW)	$P^{+}_{\rm min}$ (MW)
159	0	8.5252	−0.4198	0.6225	0.7075	0.065	0.05	1.73	1.76
159	3	8.5881	−0.5792	0.6175	0.6925	0.065	0.045	1.45	1.48
159	5	8.4325	−0.6653	0.6125	0.6825	0.055	0.045	1.31	1.33
159	7	8.4065	−0.8253	0.6075	0.6725	0.055	0.045	1.15	1.18
160	0	8.6504	−0.6349	0.6125	0.6875	0.06	0.05	1.25	1.28
160	3	8.426	−0.7314	0.6075	0.6775	0.055	0.04	1.15	1.19
160	5	8.3789	−0.9227	0.6025	0.6675	0.055	0.04	1.18	1.21
160	7	8.3289	−1.0934	0.5975	0.6575	0.05	0.04	1.21	1.24

We changed the OKCD by adjusting the EC wave starting incidence angles but maintained the co-current, which was well aligned with the target resonant magnetic surface to ascertain the counter-current inhibitory influence on NTM under different conditions. Table 3 lists the results of the calculation of the minimal EC power under the co-current and counter-current. The results when just the co-current is considered are also listed. Table 3 shows that for all results, the least power $P_{\rm min}$ needed to stabilize NTM by combining co-current and counter-current is less than the minimum power $P^{+}_{\rm min}$ when co-current alone is used. This is in line with the conclusion of Subsection 3.1. The counter-current can have some inhibitory effects on NTM if there is a significant misalignment deviation between its position and the target resonant magnetic surface.

Figure 6 shows the results of the minimum EC power calculated by the newly constructed theoretical model in this paper with (α,β). According to the results in Table 3 and Fig. 6, the optimal minimum wave power is 1.15 MW, and the two sets of initial incidental angles are ($\alpha = 159°$, $\beta = 7°$) and ($\alpha = 160°$, $\beta = 3°$), and the co-current deposition positions are all at $0.6075a$, well aligned with the $2/1$ resonant magnetic surface ($\rho_{2/1} = 0.6025a$). The deposition positions of counter-current are located at $0.6725a$ and $0.6775a$, respectively, which deviate far away from the $2/1$ resonant magnetic surface.

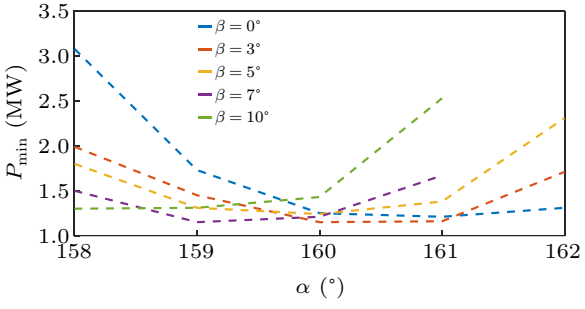


Fig. 6. The minimum EC power required to stabilize $2/1$ NTM versus initial incident angles. Both the co-current and counter-current of OKCD are considered in the calculation of the minimum EC power.

All these results indicate that even if OKCD drives co-current and counter-current under certain conditions, if the co-current can be well aligned with the target resonant magnetic surface, while the lower counter-current can maintain a sufficient deviation from this surface, the co-current and counter-current generated by OKCD can have the maximum inhibitory effect on NTM.

4. Summary and conclusion

In this paper, we construct a physical model for the counter-current to suppress the growth rate of the NTM magnetic island and obtain the modified Rutherford equation including the contributions of co-current and counter-current. Using the newly constructed modified Rutherford equation, we investigate the effect of counter-current on NTM suppression. It is discovered that only when the misalignment deviation from the target resonant magnetic surface is sufficiently significant can the counter-current partly suppress the NTM magnetic island. This is consistent with experimental results that NTM can only be partially suppressed by counter-current. The most critical factor for counter-current to suppress NTM is the ratio of counter-current misalignment deviation to current width $x \equiv |x_{\rm dep}|/w_{\rm dep}$, where the value of x should be between 0.6 and 0.8.

Under specific circumstances, co-current and counter-current can be produced by the Ohkawa mechanism dominated current drive (OKCD) of electron cyclotron wave. In this case, the counter-current with a lower peak value will diverge from the target resonant magnetic surface if the co-current with a higher peak value is well aligned with it. The co-current and counter-current of OKCD will both stabilize the growth of the NTM magnetic island if the co-current with a larger peak value is well aligned with the target resonant magnetic surface according to the modified Rutherford equation. The co-current plays a leading role, and the counter-current plays a partial inhibitory role.

The minimum EC power when considering both co–current and counter-current for the suppression of NTM is marginally lower than when considering only the co-current according to the results of multiple groups of OKCD. Since the lower counter-current also has a partially stable effect in this situation, only the co-current with the higher peak needs to be perfectly aligned with the target resonance magnetic surface when using OKCD to suppress NTM.

Appendix A

This appendix details the effective parameters $F_{\rm CD}$ and $r_{\rm s}\Delta'_{\rm H}$ in Eq. (6). This is done under the following three assumptions. First, the effect of the relative deviation from the rational surface depends on $w^* = w/w_{\rm dep}$. Second, the value of the modulation duty cycle $D_{\rm mod}$ will not affect the value of $x_{\rm dep}$ within a good approximation ($\sim 10\%$). Third, assume that $\varphi_{\rm mod} = 0$. Then, $F_{\rm CD}$ can be decomposed into[17,29,30]

$$F_{\rm CD} = N_{\rm CD}(w^*)G_{\rm CD}(w^*, x_{\rm dep})M_{\rm CD}(w^*, D_{\rm mod}). \tag{A1}$$

Among them, $N_{\rm CD}$ describes the effect of magnetic island width on $F_{\rm CD}$

$$N_{\rm CD}(w^*) = \frac{0.25 + 0.24w^*}{1 + 0.64w^{*3} + 0.43w^{*2} + 1.5w^*}. \tag{A2}$$

The $G_{\rm CD}(w^*, x_{\rm dep})$ describes the impact of misalignment effects[17,39]

$$G_{\rm CD}\left(w^*, x_{\rm dep}\right) = 1 - 2\frac{x_{\rm dep}}{g(w^*)}\,{\rm e}^{-\left(\frac{x_{\rm dep}}{g(w^*)}\right)^2}\int_0^{x_{\rm dep}/g(w^*)} {\rm d}t\,{\rm e}^{t^2}, \tag{A3}$$

wherein

$$g(w^*) = \frac{0.38w^{*2} + 0.26w^* + 0.5}{w^* + 1}. \tag{A4}$$

The $M_{\rm CD}(w^*, D_{\rm m})$ mainly considers the influence of the modulation duty cycle

$$M_{\rm CD}(w^*, D_{\rm mod}) = \frac{1}{w^{*3}}\left[m_1(D_{\rm mod})w^{*2} + m_2(D_{\rm mod})\right] + m_3(D_{\rm mod}), \tag{A5}$$

wherein

$$m_1 = 2.26D_{\rm mod}^4 - 3.44D_{\rm mod}^3 - 0.99D_{\rm mod}^2 + 2.2D_{\rm mod} - 0.02, \tag{A6}$$

$$m_2 = 0.01(0.34D_{\rm mod}^5 - 1.02D_{\rm mod}^4 + 0.87D_{\rm mod}^3 - 0.28D_{\rm mod}^2 + 0.1D_{\rm mod}), \tag{A7}$$

$$m_3 = 1.34D_{\rm mod}^4 - 3.54D_{\rm mod}^3 + 1.1D_{\rm mod}^2 + 2.09D_{\rm mod} + 0.01. \tag{A8}$$

The expression of the stabilizing effect[17,30] due to the increased heating effect of electron cyclotron waves is

$$r_{\rm s}\Delta'_{\rm H} = -\frac{16\mu_0 L_q}{B_\theta \pi}\frac{\eta_{\rm H}P_{\rm tot}}{w_{\rm dep}^2}F_{\rm H}\left(w^*, x_{\rm dep}, D_{\rm mod}, \phi_{\rm mod}\right), \tag{A9}$$

wherein $\eta_{\rm H}$ represents the drive efficiency produced by heating

$$\eta_{\rm H} = \frac{3w_{\rm dep}^2}{8\pi R n_{\rm e}\chi_\perp k_{\rm B}}\frac{j_{\rm s}}{T_{\rm s}}. \tag{A10}$$

Here $j_{\rm s} = j_\parallel - j_{\rm BS}$, $j_\parallel$ is the equilibrium current density, $T_{\rm s}$ is the electron temperature on the resonant magnetic surface, $\chi_\perp$ is the vertical thermal diffusion coefficient and $k_{\rm B}$ is Boltzmann's constant (unit: J·keV^{-1}). $F_{\rm H}$ is the effective parameter under the heating effect

$$F_{\rm H} = N_{\rm H}(w^*)G_{\rm H}(w^*, x_{\rm dep})M_{\rm H}(w^*, D_{\rm mod}), \tag{A11}$$

$$N_{\rm H}(w^*) = \frac{0.077w^{*2} + 0.088w^*}{w^{*2} + 0.8w^* + 2.17}, \tag{A12}$$

$$G_{\rm H}(w^*, x_{\rm dep}) = \exp\left[-\left(\frac{x_{\rm dep}}{g(w^*)}\right)^2\right], \tag{A13}$$

wherein

$$g(w^*) = 0.00035w^{*4} - 0.008w^{*3} + 0.07w^{*2} + 0.02w^* + 0.5, \tag{A14}$$

$$M_{\rm H}(w^*, D_{\rm mod}) = 1.2D_{\rm mod}^3 - 3.5D_{\rm mod}^2 + 3.3D_{\rm mod} - 0.06. \tag{A15}$$

Data availability statement

The data that support the findings of this study are openly available in Science Data Bank at the following link https://doi.org/10.57760/sciencedb.j00113.00205

Acknowledgments

Project supported by the National Key R&D Program of China (Grant Nos. 2022YFE03070000 and 2022YFE03070003), the National Natural Science Foundation of China (Grant Nos. 12375220 and 12075114), the Hunan Provincial Natural Science Foundation (Grant No. 2021JJ30569), the Doctoral Initiation Fund Project of University of South China (Grant No. 190XQD114), the Hunan Nuclear Fusion International Science and Technology Innovation Cooperation Base (Grant No. 2018WK4009), and the Hengyang Key Laboratory of Magnetic Confinement Nuclear Fusion Research (Grant No. 2018KJ108).

References

[1] Prater R 2004 *Phys. Plasmas* **11** 2349
[2] Igochine V 2015 *Active Control of Magneto-hydrodynamic Instabilities in Hot Plasmas* (Berlin: Springer Berlin Heidelberg) pp. 83–85
[3] Haye R J L 2006 *Phys. Plasmas* **13** 055501
[4] Pietrzyk Z A, Angioni C, Behn R, Coda S, Goodman T P, Henderson M A, Hofmann F and Sauter O 2001 *Phys. Rev. Lett* **86** 1530
[5] Petty C C, La Haye R J, Luce T C, Humphreys D A, Hyatt A W, Lohr J, Prater R, Strait E J and Wade M R 2004 *Nucl. Fusion* **44** 243
[6] Prater R, La Haye R J, Luce T C, Petty C C, Strait E J, Ferron J R, Humphreys D A, Isayama A, Lohr J, Nagasaki K, Politzer P A, Wade M R and Welander A S 2007 *Nucl. Fusion* **47** 371
[7] Kolemen E, Welander A S, La Haye R J, Eidietis N W, Humphreys D A, Lohr J, Noraky V, Penaflor B G, Prater R and Turco F 2014 *Nucl. Fusion* **54** 073020
[8] Isayama A, Matsunaga G, Kobayashi T, Moriyama1 S, Oyama N, Sakamoto1 Y, Suzuki T, Urano H, Hayashi N, Kamada Y, Ozeki T, Hirano Y, Urso L, Zohm H, Maraschek M, Hobirk J, Nagasaki K and the JT-60 team 2009 *Nucl. Fusion* **49** 055006

[9] Maraschek M, Gantenbein G, Yu Q, Zohm H, Günter S, Leuterer F and Manini F 2007 *Phys. Rev. Lett* **98** 025005

[10] Warrick C D, Buttery R J, Cunningham G, Fielding S J, Hender T C, Lloyd B, Morris A W, O'Brien M R, Pinfold T, Stammers K, Valovic M, Walsh M, Wilson H R, COMPASS-D and RF teams 2000 *Phys. Rev. Lett* **85** 574

[11] Reiman A H and Fisch N J 2018 *Phys. Rev. Lett* **121** 225001

[12] Yu Q, Günter S and Lackner K 2018 *Nucl. Fusion* **58** 054003

[13] Wang Z X, Tang W K and Wei L 2022 *Plasma Sci. Technol* **24** 033001

[14] Tang W K, Wang Z X, Wei L, Wang J L and Lu S S 2020 *Nucl. Fusion* **60** 026015

[15] Liu T, Wang Z X, Wei L and Wang J L 2022 *Nucl. Fusion* **62** 056018

[16] Poli E, Angioni.C, Casson F J, Farina D, Figini L, Goodman T P, Maj O, Sauter O, Weber H, Zohm H, Saibene G and Henderson M A 2015 *Nucl. Fusion* **55** 013023

[17] De Lazzari D and Westerhof E 2009 *Nucl. Fusion* **49** 075002

[18] La Haye R J, Ferron J R, Humphreys D A, Luce T C, Petty C C, Prater R, Strait E J and Welander A S 2008 *Nucl. Fusion* **48** 054004

[19] He L H, Zheng P W and Yu T 2023 *Nucl. Eng. Technol* **55** 2941

[20] Kong M, Blanken T C, Felici F, Galperti C, Maljaars E, Sauter O, Vu1 T, Carpanese F, Merle A, Moret J M, Pesamosca F, Poli E, Reich M, Teplukhina A, The TCV Team and The EUROfusion MST Team 2019 *Nucl. Fusion* **59** 076035

[21] Maraschek M 2012 *Nucl. Fusion* **52** 074007

[22] Shi M L, Zheng P W, Yin L, He H L, Hua Q H, Zhong Y J, Deng S and Gong X Y 2022 *Plasma Phys. Control. Fusion* **64** 115013

[23] Park Y S 2008 *J. Korean Phys. Soc.* **53** 1923

[24] Lu S S, Liu Y and Wei L 2020 *Vacuum* **182** 109656

[25] Jenkins, T G, Kruger, S E, Hegna, C C, Schnack, DD and Sovinec C R 2010 *Phys. Plasmas* **17** 012502

[26] Février O, Maget P, Lütjens H, Luciani J F, Decker J, Giruzzi G, Reich M, Beyer P, Lazzaro E, Nowak S and the ASDEX Upgrade team 2016 *Plasma Phys. Control. Fusion* **58** 045015

[27] Wang X J, Yu Q Q, Zhang X D, Zhang Y, Zhu S Z, Wang X G and Wu B 2018 *Plasma Phys. Control. Fusion* **60** 045004

[28] Westerhof E, Blank H J de and Pratt J 2016 *Nucl. Fusion* **56** 036016

[29] Bertelli N, De Lazzari D and Westerhof E 2011 *Nucl. Fusion* **51** 103007

[30] De Lazzari D and Westerhof E 2010 *Nucl. Fusion* **50** 079801

[31] Sautor O, Henderson M A, Ramponi G, Zohm H and Zucca C 2010 *Plasma Phys. Control. Fusion* **52** 025002

[32] La Haye R J, Prater R, Buttery R J, Hayashi N, Isayama A, Maraschek M E, Urso L and Zohm H 2006 *Nucl. Fusion* **46** 451

[33] Li C Y, Zheng P W, Jiang X C, Lu L F, Yin L, He L H, Huang Q H, Zhong Y J and Gong X Y 2022 *Nucl. Fusion* **62** 096027

[34] Zheng P W, Gong X Y, Lu X Q, He L H, Cao J J, Huang Q H and Deng S 2018 *Nucl. Fusion* **58** 036010

[35] Zheng P W, Gong X Y, Lu X Q, Cao J J, He L H, Huang Q H, Deng S, Lin J F and Zhong Y J 2018 *Plasma Phys* **25** 072501

[36] Smirnov A P, Harvey R W and Prater R 2009 *World Scientific* EC-15 301

[37] Harvey R W and McCoy M G 1992 *Proceedings of the IAEA Technical Committee Meeting on Simulation and Modeling of Thermonuclear Plasmas*, June 5–18,1992, Montreal, Canada, p. 489

[38] Petrov Y V and Harvey R W 2016 *Plasma Phys. Control. Fusion* **58** 115001

[39] Poli F M, Fredrickson E D, Henderson M A, Kim S H, Bertelli N, Poli E, Farina D and Figini L 2018 *Nucl. Fusion* **58** 016007